EQUATION OF STATE, CORRELATIONS AND FLUCTUATIONS FROM LATTICE QCD*

Claudia Ratti[a], Szabolcs Borsanyi[b], Gergely Endrődi[c]
Zoltan Fodor[b,d,e], Sandor Katz[d], Stefan Krieg[b,e]
Kalman Szabo[b]

[a]Università degli Studi di Torino e INFN, Sezione di Torino
via P. Giuria 1, 10125 Torino, Italy
[b]Department of Physics, Wuppertal University
Gaussstr. 20, 42119 Wuppertal, Germany
[c]Institut für Theoretische Physik, Regensburg University
Universitätsstr. 31, 93040 Regensburg, Germany
[d]Institute for Theoretical Physics, Eötvös University
Pázmány 1, 1117 Budapest, Hungary
[e]Jülich Supercomputing Centre
Forschungszentrum Jülich, 52425 Jülich, Germany

(Received January 2, 2012)

We conclude our investigation on the QCD equation of state (EoS) with $2+1$ staggered flavors and one-link stout improvement. We extend our previous study by choosing even finer lattices. These new results support our earlier findings. Lattices with $N_t = 6, 8$ and 10 are used, and the continuum limit is approached by checking the results at $N_t = 12$. A Symanzik improved gauge and a stout-link improved staggered fermion action is taken; the light and strange quark masses are set to their physical values. Various observables are calculated in the temperature (T) interval of 100 to 1000 MeV. We also present our new results on flavor diagonal and non-diagonal quark number susceptibilities, in a temperature regime between 120 and 400 MeV. In this case, lattices with $N_t = 6,\ 8,\ 10,\ 12$ are used. We perform a continuum extrapolation of those observables for which the scaling regime is reached, and discretization errors are under control.

DOI:10.5506/APhysPolBSupp.5.837
PACS numbers: 11.15.Ha, 12.38.Gc

* Talk presented at HIC for FAIR Workshop and XXVIII Max Born Symposium "Three Days on Quarkyonic Island", Wrocław, Poland, May 19–21, 2011.

1. Introduction

The study of QCD thermodynamics and that of the phase diagram are receiving increasing attention in recent years. A transition occurs in strongly interacting matter from a hadronic, confined system at small temperatures and densities to a phase dominated by colored degrees of freedom at large temperatures or densities. A systematic approach to determine properties of this transition is through lattice QCD. Lattice simulations indicate that the transition at vanishing chemical potential is merely an analytic crossover [1]. This field of physics is particularly appealing because the deconfined phase of QCD can be produced in the laboratory, in the ultrarelativistic heavy ion collision experiments at CERN SPS, RHIC at Brookhaven National Laboratory, ALICE at the LHC and the future FAIR at the GSI. The experimental results available so far show that the hot QCD matter produced experimentally exhibits robust collective flow phenomena, which are well and consistently described by near-ideal relativistic hydrodynamics. These hydrodynamical models need as an input an EoS which relates the local thermodynamic quantities.

Most of the results on the QCD EoS have been obtained using improved staggered fermions. This formulation does not preserve the flavor symmetry of continuum QCD; as a consequence, the spectrum of low lying hadron states is distorted. Recent analyses performed by various collaborations [2,3] have pointed out that this distortion can have a dramatic impact on the thermodynamic quantities. To quantify this effect, one can compare the low temperature behavior of the observables obtained on the lattice, to the predictions of the Hadron Resonance Gas (HRG) model.

A lot of effort is invested, both theoretically and experimentally, in order to find observables which would unambiguously signal the QCD phase transition. Correlations and fluctuations of conserved charges have been proposed long ago to this purpose [4, 5]. The idea is that these quantum numbers have a very different value in a confined and deconfined system, and measuring them in the laboratory would allow to distinguish between the two phases. Fluctuations of conserved charges can be obtained as linear combinations of diagonal and non-diagonal quark number susceptibilities, which can be calculated on the lattice at zero chemical potential [6, 3].

In the present contribution, we show the results of our collaboration on some of these observables, with 2+1 staggered quark flavors, in a temperature regime between 100 and 1000 MeV for the EoS, and between 120 and 400 MeV for the susceptibilities. The light and strange quark masses are set to their physical values. Lattices with $N_t = 6,\ 8,\ 10,\ 12$ are used. Continuum extrapolations are performed for those observables for which discretization errors are under control and the scaling regime is reached.

2. Lattice framework

The lattice action is the same as we used in [7, 8], namely a tree-level Symanzik improved gauge, and a stout-improved staggered fermionic action (see Ref. [9] for details). The stout-smearing [10] reduces the taste violation: this kind of smearing has one of the smallest taste violation among the ones used so far in the literature, together with the hisq action recently proposed by the hotQCD Collaboration [11,12]. Here we present our results for thermodynamic observables: pressure (p), trace anomaly ($I = \epsilon - 3p$) and speed of sound ($c_{\rm s}$), for $n_f = 2 + 1$ dynamical quarks. We also present our most recent results on quark number susceptibilities [13]. We improve our previous findings [9] by choosing finer lattices ($N_t = 8,\ 10$ and a few checkpoints at $N_t = 12$). We work again with physical light and strange quark masses: we fix them by reproducing the physical ratios f_K/m_π and f_K/m_K and by this procedure [3,8,14] we get $m_s/m_{u,d} = 28.15$. We checked that there were no significant finite size effects by performing two sets of simulations in boxes with a size of 3.5 fm and 7 fm around $T_{\rm c}$. The left panel of figure 1 shows the comparison between the two volumes for the normalized trace anomaly I/T^4. Let us note here, that the volume independence in the transition region is an unambiguous evidence for the crossover type of the transition.

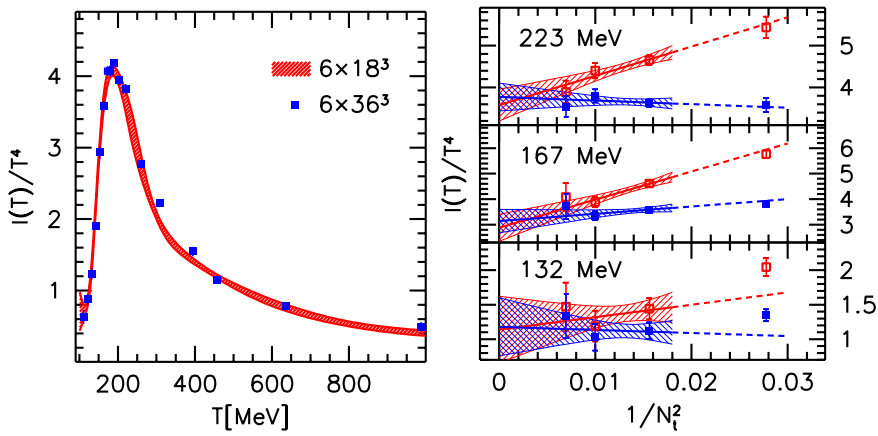

Fig. 1. Left: The trace anomaly on lattices with different spatial volumes: $N_s/N_t = 3$ (gray/red band) and $N_s/N_t = 6$ (black/blue points). Right: $I = \epsilon - 3p$ at three different Ts as a function of $1/N_t^2$. Filled/open symbols represent results with/without tree-level improvement.

To decrease lattice artefacts, we apply tree-level improvement for our thermodynamic observables: we divide the lattice results with the appropriate improvement coefficients. These factors can be calculated analytically for our action and, in case of the pressure, we have the following values on different N_ts: $N_t = 6$ gives 1.517, $N_t = 8$ gives 1.283, $N_t = 10$ gives 1.159 and $N_t = 12$ gives 1.099. Using thermodynamical relations one can obtain these improvement coefficients for the energy density, trace anomaly and entropy, as well as for the susceptibilities. The speed of sound receives no improvement factor at tree level. Note, that these improvement coefficients are exact only at tree-level, thus in the infinitely high temperature, non-interacting case. As we decrease the temperature, corrections to these improvement coefficients appear, which have the form $1 + b_2(T)/N_t^2 + \ldots$. Empirically, one finds that the $b_2(T)$ coefficient, which describes the size of lattice artefacts of the tree-level improved quantities, is tiny not only at very high temperatures, but throughout the deconfined phase. The right panel of figure 1 illustrates at three temperature values ($T = 132$, 167 and 223 MeV) the effectiveness of this improvement procedure. We show both the unimproved/improved values of the trace anomaly for $N_t = 6, 8, 10$ and 12 as a function of $1/N_t^2$. The lines are linear continuum extrapolations using the three smallest as. The $a \to 0$ limit of both the unimproved and the improved observables converge to the same value. The figure confirms the expectations, that lattice tree-level improvement effectively reduces the cutoff effects. At all three Ts, the unimproved observables have larger cutoff effects than the improved ones. Actually, all the three values of $b_2(T)$, which indicate the remaining cutoff effects after tree-level improvement, differ from zero by less than one standard deviation.

The most popular technique to determine the EoS is the integral method. For large homogeneous systems, p is proportional to the logarithm of the partition function. Its direct determination is difficult. Instead, one determines the partial derivatives with respect to the bare lattice parameters. Finally, p is rewritten as a multidimensional integral along a path in the space of bare parameters. To obtain the EoS for various m_π, we simulate for a wide range of bare parameters on the plane of $m_{u,d}$ and β (m_s is fixed to its physical value). Having obtained this large set of data we generalize the integral method and include all possible integration paths into the analysis [15, 16].

An additive divergence is present in p, which is independent of T. One removes it by subtracting the same observables measured on a lattice, with the same bare parameters but at a different T value. Here we use lattices with a large enough temporal extent, so it can be regarded as $T = 0$.

3. Results

3.1. Equation of state

As we will see, different sets of data corresponding to different N_t nicely agree with each other for all observables under study: thus, we expect that discretization effects are tiny.

In the left panel of figure 2 we show the T dependence of $\epsilon - 3p$ for $n_f = 2 + 1$. We have results at four different as. Results show essentially no dependence on a, they all lie on top of each other. Only the coarsest $N_t = 6$ lattice shows some deviation around $\sim 300\,\mathrm{MeV}$. In the same figure, we zoom in to the transition region. Here, we also show the results from the HRG model: a good agreement with the lattice results is found up to $T \sim 140\,\mathrm{MeV}$. One characteristic temperature of the crossover transition can be defined as the inflection point of the trace anomaly. This and other characteristic features of the trace anomaly are the following: the inflection point of $I(T)/T^4$ is 152(4) MeV; the maximum value of $I(T)/T^4$ is 4.1(1), whereas T at the maximum of $I(T)/T^4$ is 191(5) MeV.

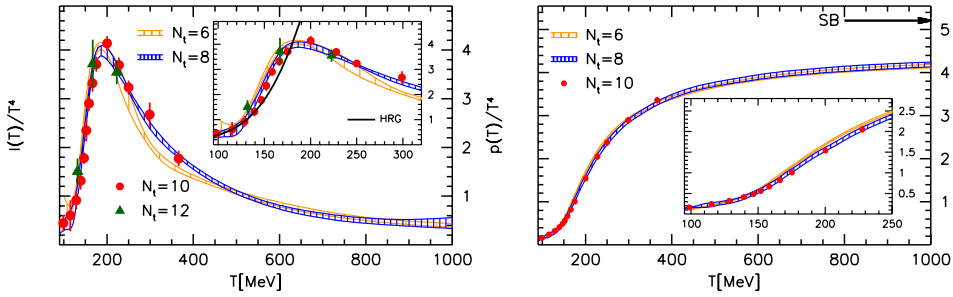

Fig. 2. Left: The trace anomaly normalized by T^4 as a function of T on $N_t = 6, 8, 10$ and 12 lattices. Right: $p(T)$ normalized by T^4 as a function of the temperature on $N_t = 6, 8$ and 10 lattices. The Stefan–Boltzmann limit $p_{\mathrm{SB}}(T) \approx 5.209 \times T^4$ is indicated. At $T = 1000\,\mathrm{MeV}$ $p(T)$ is almost 20% below this limit.

In the right panel of figure 2 we show $p(T)$. We have results at three different as. The $N_t = 6$ and $N_t = 8$ are in the T range from 100 up to 1000 MeV. In the left panel of figure 3 we present the energy density. In the right panel of figure 3 $c_{\mathrm{s}}^2(T)$, the speed of sound is shown. One can also read off the characteristic points of this curve: the minimum value of $c_{\mathrm{s}}^2(T)$ is 0.133(5); T at the minimum of $c_{\mathrm{s}}^2(T)$ is 145(5) MeV; whereas ϵ at the minimum of $c_{\mathrm{s}}^2(T)$ is 0.20(4) GeV/fm^3.

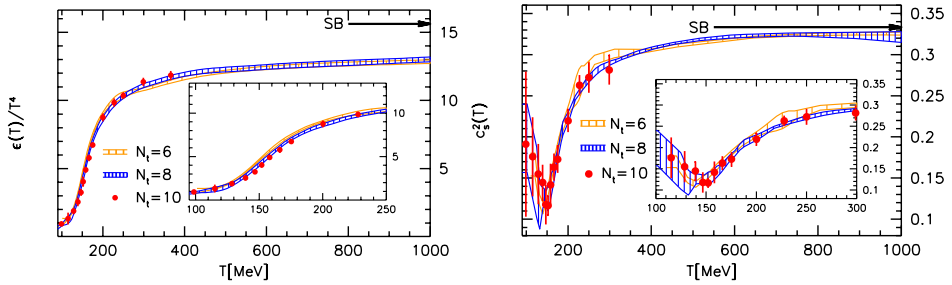

Fig. 3. Left: The energy density normalized by T^4 as a function of temperature on $N_t = 6, 8$ and 10 lattices. The Stefan–Boltzmann limit $\epsilon_{\rm SB} = 3p_{\rm SB}$ is indicated by an arrow. Right: The speed of sound squared as a function of temperature on $N_t = 6, 8$ and 10 lattices. The Stefan–Boltzmann limit is $c^2_{s,\rm SB} = 1/3$ indicated by an arrow.

3.2. Susceptibilities

Quark number susceptibilities are defined as derivatives of the QCD pressure with respect to the quark chemical potentials. In particular, we consider the following ones

$$c_2^{uu} = \frac{T}{V}\frac{\partial^2 \ln Z}{\partial\mu_u\partial\mu_u}\bigg|_{\mu_i=0}, \quad c_2^{us} = c_2^{ds} = \frac{T}{V}\frac{\partial^2 \ln Z}{\partial\mu_u\partial\mu_s}\bigg|_{\mu_i=0}, \quad \chi_2^s = \frac{T}{V}\frac{\partial^2 \ln Z}{\partial\mu_s\partial\mu_s}\bigg|_{\mu_i=0}. \tag{1}$$

In the left panel of Fig. 4 we show the diagonal light quark susceptibility as a function of temperature. Results are obtained on five different lattices: $N_t = 6,\ 8,\ 10$ and two different spatial volumes for $N_t = 12$: 32^3 and 36^3. This observable reaches approximately 90% of the Stefan–Boltzmann limit already at $T \sim 400\,$MeV. Notice that we do not perform a continuum extrapolation: this observable is pion-dominated at small temperatures and we need either finer lattices or an action which reduces even more the taste violation, in order to reach the scaling regime and give the correct continuum estimate. In the right panel of Fig. 4 we show the non-diagonal $u - s$ susceptibility, which measures the correlation between these different flavors. As we can see, this observable has a peak in the vicinity of the phase transition, and tends to zero for infinitely large temperatures. This observable is very noisy and before performing a continuum extrapolation we need to reduce the errorbars for the $N_t = 12$ sets of data. A quantitative comparison between lattice results and predictions for a purely partonic QGP state can give us information about the probability of bound states survival above $T_{\rm c}$: recent investigations in this direction [20] seem to indicate that there is a certain temperature range above $T_{\rm c}$, where bound states give a relevant contribution to this observable.

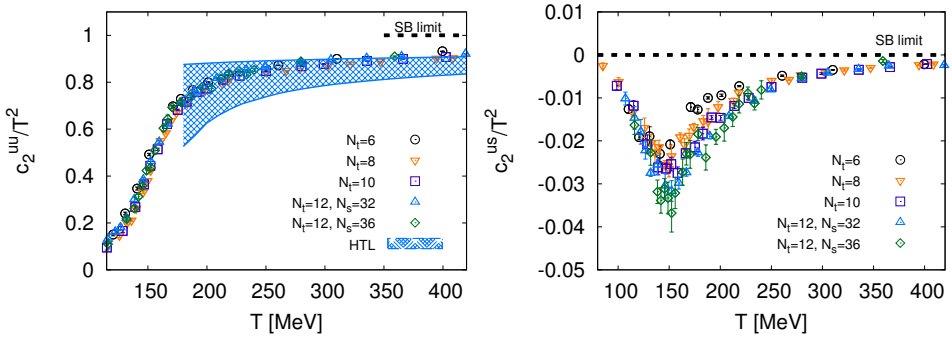

Fig. 4. Left: Diagonal light quark susceptibility as a function of temperature. Right: Non-diagonal $u-s$ susceptibility as a function of temperature. In both panels, data are obtained on $N_t = 6,\ 8,\ 10$ and 12 lattices. Two different spatial volumes are considered for the latter: 32^3 and 36^3. The band in the left panel is the comparison with the Hard Thermal Loop predictions taken from Ref. [19].

In the left panel of Fig. 5 we show the strange quark number susceptibility as a function of the temperature. For this observable we perform a continuum extrapolation, as well as a comparison to the HRG model predictions. In the right panel of Fig. 5 we show, for $N_t = 12$, a comparison between light and strange susceptibilities. We notice that the rapid rise as a function of the temperature occurs at larger temperatures for strange quarks than for light quarks.

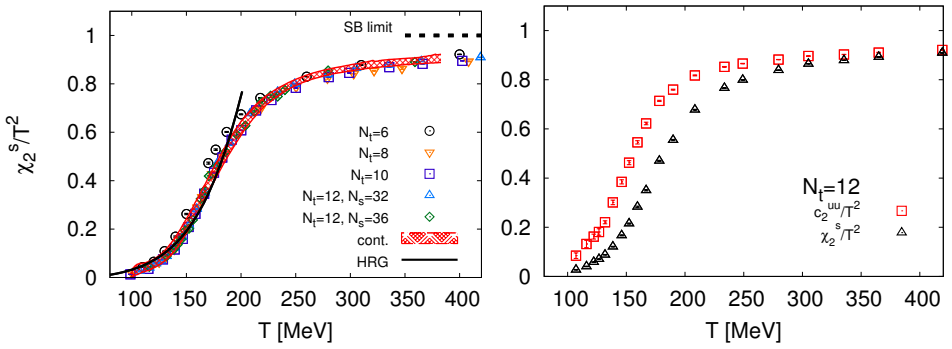

Fig. 5. Left: Diagonal strange quark susceptibility as a function of temperature. Data are obtained on $N_t = 6,\ 8,\ 10$ and 12 lattices. Two different spatial volumes are considered for the latter: 32^3 and 36^3. The gray (red) band indicates the continuum extrapolation. The black curve is the Hadron Resonance Gas (HRG) model prediction. Right: Comparison between the light and strange quark susceptibility as functions of the temperature, for $N_t = 12$.

Baryon number susceptibility is defined as a linear combination of quark number susceptibilities in the following way

$$\chi_B = \frac{1}{9}\left(2c_2^{uu} + \chi_2^s + 2c_2^{ud} + 4c_2^{us}\right), \quad \text{with} \quad c_2^{ud} = \frac{T}{V}\frac{\partial^2 \ln Z}{\partial\mu_u \partial\mu_d}\bigg|_{\mu_i=0}. \quad (2)$$

We show our results for this observable in the left panel of Fig. 6: a continuum extrapolation is performed, and compared to the HRG model results. The agreement is very good. In the right panel of Fig. 6 we show the baryon–strangeness correlator that was proposed in Ref. [21] as a diagnostic of strongly interacting matter. It is defined as

$$C_{\rm BS} = 1 + \frac{c_2^{us} + c_2^{ds}}{\chi_2^s}. \quad (3)$$

The continuum extrapolation is in good agreement with the HRG model prediction for temperatures smaller than $T_{\rm c}$.

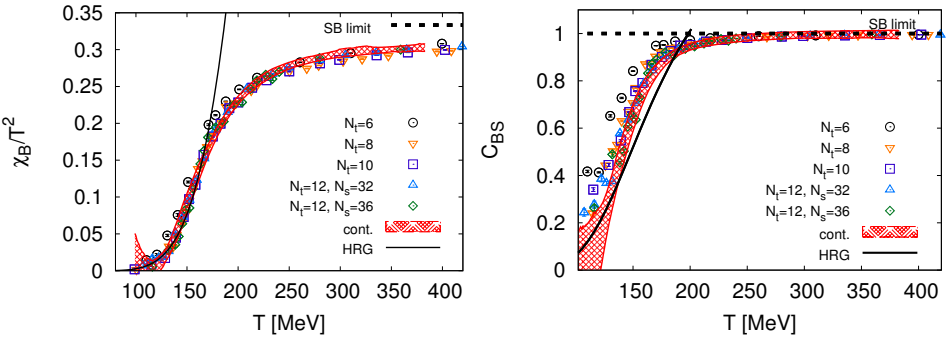

Fig. 6. Left: Baryon number susceptibility as a function of temperature. Right: Baryon–strangeness correlator as a function of the temperature. In both panels, results for $N_t = 6,\ 8,\ 10$ and 12 lattices are shown. Two different spatial volumes are considered for the latter: 32^3 and 36^3. The gray (red) band is the continuum extrapolated result, the black curve is the prediction of the HRG model.

4. Conclusions

We determined the equation of state and second order quark number susceptibilities of QCD by means of lattice simulations. Results for the $n_f = 2 + 1$ flavor pressure, trace anomaly, speed of sound, light and strange diagonal and non-diagonal susceptibilities were presented in figures, together with baryon number susceptibilities and baryon–strangeness correlations.

The results were obtained by carrying out lattice simulations at four different as, at $N_t = 6, 8, 10$ and 12 in the T range of $T = 100 \ldots 1000$ MeV for the EoS and $T = 120 \ldots 400$ MeV for the susceptibilities. In order to reduce the lattice artefacts we applied tree-level improvement for all of the thermodynamical observables. We found that there is no difference in the results at the three finest lattice spacings. This shows that the lattice discretization errors are not significant and the continuum limit can be reliably taken.

Work supported in part by the EU grant (FP7/2007-2013)/ERC no. 208740. The work of C.R. is supported by funds provided by the Italian Ministry of Education, Universities and Research under the Firb Research Grant RBFR0814TT.

REFERENCES

[1] Y. Aoki *et al.*, *Nature* **443**, 675 (2006).

[2] P. Huovinen, P. Petreczky, *Nucl. Phys.* **A837**, 26 (2010) [arXiv:0912.2541v2 [hep-ph]].

[3] S. Borsanyi *et al.* [Wuppertal–Budapest Collaboration], *J. High Energy Phys.* **1009**, 073 (2010).

[4] S. Jeon, V. Koch, *Phys. Rev. Lett.* **85**, 2076 (2000).

[5] M. Asakawa, U.W. Heinz, B. Muller, *Phys. Rev. Lett.* **85**, 2072 (2000).

[6] A. Bazavov *et al.*, *Phys. Rev.* **D80**, 014504 (2009); S. Mukherjee, arXiv:1107.0765v1 [nucl-th].

[7] Y. Aoki, Z. Fodor, S.D. Katz, K.K. Szabo, *Phys. Lett.* **B643**, 46 (2006).

[8] Y. Aoki *et al.*, *J. High Energy Phys.* **0906**, 088 (2009).

[9] Y. Aoki, Z. Fodor, S.D. Katz, K.K. Szabo, *J. High Energy Phys.* **0601**, 089 (2006).

[10] C. Morningstar, M.J. Peardon, *Phys. Rev.* **D69**, 054501 (2004).

[11] A. Bazavov, P. Petreczky, *PoS* **LAT2009**, 163 (2009).

[12] A. Bazavov, P. Petreczky, *J. Phys. Conf. Ser.* **230**, 012014 (2010) [arXiv:1005.1131v1 [hep-lat]].

[13] S. Borsanyi *et al.* [Wuppertal–Budapest Collaboration], arXiv:1109.5030v1 [hep-lat].

[14] Y. Aoki, Z. Fodor, S.D. Katz, K.K. Szabo, *Phys. Lett.* **B643**, 46 (2006).

[15] S. Borsanyi *et al.*, *J. High Energy Phys.* **1011**, 077 (2010) [arXiv:1007.2580v2 [hep-lat]].

[16] G. Endrodi, arXiv:1010.2952v2 [physics.comp-ph].

[17] A. Bazavov *et al.*, *Phys. Rev.* **D80**, 014504 (2009).

[18] M. Cheng *et al.*, *Phys. Rev.* **D81**, 054504 (2010).

[19] J.P. Blaizot, E. Iancu, A. Rebhan, *Phys. Lett.* **B523**, 143 (2001) [arXiv:hep-ph/0110369v3].

[20] C. Ratti, R. Bellwied, M. Cristoforetti, M. Barbaro, arXiv:1109.6243v1 [hep-ph].

[21] V. Koch, A. Majumder, J. Randrup, *Phys. Rev. Lett.* **95**, 182301 (2005).